PHYSICAL REVIEW B VOLUME 22, NUMBER 8 15 OCTOBER 1980

Extended x-ray absorption fine-structure determinations of coordination numbers: Limitations

P. Eisenberger
Bell Laboratories, Murray Hill, New Jersey 07974

B. Lengeler
Institut für Festkorperforschung, Kernforschungsanlage Jülich, 5170 Jülich, Federal Republic of Germany
(Received 7 February 1980)

Comparisons are made between measured extended x-ray absorption fine-structure (EXAFS) amplitudes for nearest- and more-distant-neighbor coordination shells in a wide variety of known compounds at both room temperature and 77 K. The comparisons reveal a significant sensitivity of the amplitudes to the chemical environment and non-Gaussian disorder. The observed changes can cause significant errors in the empirical determinations of coordination numbers. The absence of the possibility of a quantitative theoretical calculation of the EXAFS amplitude leads to the conclusion that coordination numbers can be determined most accurately by the use of a chemically and structurally similar model measured at low temperature.

The extended x-ray absorption fine-structure (EXAFS) technique is thought to have the possibility of determining in unknown compounds the bond lengths,[1] coordination number,[2] chemical type,[3] and, by use of polarization properties, the coordination geometry.[4] In short, a complete local structural determination is in principle possible. Only the first and last have been demonstrated in a general way. In this work we will evaluate the ability of the EXAFS technique to determine the second and third structural properties. The focus will be upon situations of known chemical constituents where only bond lengths and coordination numbers are desired, but the discussion will include the case of completely unknown structures.

It is now widely accepted that the EXAFS technique can determine to an accuracy of 0.02 Å the bond lengths in unknown materials by both empirical[1] and theoretical approaches.[5] The power of the technique is significantly attributable to the independence of the determination on chemical environment, the so-called chemical transferability of the scattering phase shifts.[1] However, recently it has been shown[6] that an asymmetric pair-distribution function between the central absorbing atom and the coordination shell of interest can introduce significant errors in the distance determinations. However, a perturbative-type corrective procedure has been developed[6] to correct for the case of small asymmetries. For large asymmetries a modeling approach is required[7] and therefore for those cases EXAFS has lost its ability to directly determine interatomic distances.

In spite of the use of EXAFS amplitudes to specify coordination numbers in systems with known constituents[2] or to identify both the chemical constituents and coordination numbers in unknown chemical environments,[3] no systematic study has been performed to evaluate the accuracy of those determinations.

In this study a large number of simple known structures were measured both at room temperature and at 77 K. Systems with the same absorbing atom and scattering atom pairs in the same coordination shells are compared as a function of the temperature and the chemical environment. In addition, the amplitudes are compared for materials with the same crystal structure and the same scattering atom but different transition-metal absorbing atoms. It will be shown that the simple and predictive EXAFS formalism cannot account for the observed changes. A complete and model-dependent formalism certainly has enough degrees of freedom to explain the observed changes but has in the process lost its predictive ability. The conclusion is reached that only the use of a chemical similar system as a model, ideally the sample itself, or a limited model-dependent fitting procedure can be successfully used to accurately determine coordination numbers and chemical constituents.

In Sec. I is developed the theoretical expression for the EXAFS amplitudes, including the evolution from the simplistic initial expressions to the current complex version. In Sec. II are described the experimental technique and data-analysis procedures. In Sec. III the experimental results are presented and, finally, in Sec. IV is presented a discussion of the conclusion of this work.

I. EXAFS FORMALISM

The formula to describe the EXAFS for an s-p transition in an absorbing atom A, surrounded by a coordination shell of N_B atoms B, with a

Gaussian pair-distribution function characterized by the standard deviation σ_{AB} is given by

$$\chi(k) = -\frac{N_B}{\bar{r}_{AB}^2 k} f_B(k,\pi)\, e^{-2k^2\sigma^2} AB \sin(2k\bar{r}_{AB} + \phi_{AB}). \quad (1)$$

In Eq. (1) k is the wave vector of ejected electron, $\bar{r}_{AB}$ is the average distance between atoms A and B, $f_B(k,\pi)$ is elastic backscattering amplitude of atoms B, and ϕ_{AB} is the total of twice the absorbing atom A and backscattering atom B phase shifts. It is assumed in Eq. (1) that the sample contains no long-range orientational order.

Equation (1) although frequently used is still recognized to contain several oversimplifications. As recently described,[6] if the pair correlation function $g_{AB}(r)$ is not symmetric, Eq. (1) takes the form

$$\chi(k) = -\frac{N_B}{\bar{r}_{AB}^2 k} f_B(k,\pi)[S_{AB}^2(k,\bar{r}_{AB},T) + A_{AB}^2(k,\bar{r}_{AB},T)]^{1/2} \times \sin[2k\bar{r}_{AB} + \phi_{AB}(k) + \sum_{AB}(k,\bar{r}_{AB},T)], \quad (2)$$

where

$$\sum_{AB}(k,\bar{r}_{AB},T) = \tan^{-1}\frac{A_{AB}(k,\bar{r}_{AB},T)}{S_{AB}(k,\bar{r}_{AB},T)}$$

and

$$S_{AB}(k,\bar{r}_{AB},T) = \int_{-\infty}^{\infty} \frac{g(\bar{r}_{AB},x,T)\cos(2kx)dx}{(1+x/\bar{r}_{AB})^2},$$

$$A_{AB}(k,\bar{r}_{AB},T) = \int_{-\infty}^{\infty} \frac{g(\bar{r}_{AB},x,T)\sin(2kx)dx}{(1+x/\bar{r}_{AB})^2},$$

and

$$\bar{r} - r = x.$$

Note that in Eq. (2) the simple separation between amplitude and phase which existed in Eq. (1) no longer exists. The implications of this for distance determinations were previously discussed.[6] The impact of Eq. (2) on coordination-number determinations will be discussed shortly.

Equation (2) still does not account for the effect of inelastic processes. There are four types of inelastic processes which diminish the size of the EXAFS amplitude. The first is caused by multiple excitations. Except in special circumstances, multiple excitations are thought to have a broad spectrum which will wash out the EXAFS signal. As shown by several authors[5,8] this loss can be related to the overlap between the ground-state and excited-state many-body wave functions. In principle, one must add the amplitudes for the various loss processes which have the same final state of the many-body system and then must square the sum to obtain the loss in intensity of the EXAFS. We will ignore this complication for our phenomenological EXAFS formula. We denote the losses upon excitation by $E_A^M(k)$, where $0 \leq E_A^M(k) \leq 1$, and where the superscript M indicates a possible dependence upon the medium in which atom A is embedded.

The other losses correspond to processes in which the emitted photoelectron excites other electrons or plasmons in moving through the charge associated with atom A, $L_A^M(k)$, the charge associated with atom B, $L_B^M(k)$, and the charge associated with the rest of the medium $L^M(k,\bar{r}_{AB})$. Here again $L_A^M(k)$, $L_B^M(k)$, and $L^M(k,\bar{r}_{AB})$ have k-dependent values between zero and one.

It would be tempting to express the product $L_A^M(k)L_B^M(k)L^M(k,\bar{r}_{AB})$ by an exponential decay $e^{-2\bar{r}_{AB}/\lambda(k)}$. However, for nearest-neighbor coordination shells the *gedanken experiment* of taking a molecule and separating the atoms would not result in increased losses nor justify a change in $\lambda(k)$ if the charges were fixed. On the other hand, for more distant shells one might expect that $L^M(k,\bar{r}_{AB})$ would have an exponential decay of the form given above. One other comment deserves mentioning concerning these losses. The losses are dominated by the weakly bound conduction and valence electrons which are sensitive to the chemical environment, while the phase shifts are dominated by the strongly bound electrons which are chemically insensitive. Thus one might expect that ϕ_{AB} and $f(k,\pi)$ would be transferable except possibly for the first-row elements, while

$$TL_{AB}^M(k,\bar{r}_{AB}) = L_A^M(k)L_B^M(k)L^M(k,\bar{r}_{AB}), \quad (3)$$

and possibly $E_A^M(k)$ would not be transferable.

Thus finally one has for the complete phenomenological formula for the EXAFS amplitude

$$|\chi(k)| = \frac{N_B}{\bar{r}_{AB}^2 k} f_B(k,\pi) E_A^M(k) TL_{AB}^M(k,\bar{r}_{AB}) \times [S_{AB}^2(k,\bar{r}_{AB},T) + A_{AB}^2(k,\bar{r}_{AB},T)]^{1/2}. \quad (4)$$

II. EXPERIMENTAL TECHNIQUE

The measurements reported in this work were made at the Standard Synchrotron Radiation Laboratory on the focussed beamline with the mirror adjusted to reduce the vertical acceptance in order to improve the energy resolution by a factor of 2. The combination of the use of a mirror and a (111) crystal made higher harmonics negligible. The

samples were measured in transmission with the thicknesses chosen to correspond to an attenuation of e^{-2} above the absorption edge. The samples were mounted on aluminum holders which could be quickly inserted into either a room-temperature mount or a nitrogen-cooled mount. The mounts were serially located in the beam path so that one could switch from one holder to another without introducing any systematic errors. The ln of the ratio of the incident to the transmitted intensity as a function of photon energy is obtained in the standard way[9] and a representative example is plotted in Fig. 1. The data jump at the edge is determined and the smooth background is removed. The EXAFS signal so determined is multiplied by either k^2 or k^3 depending upon the atomic number of the backscattering atom B and divided by a function characteristic of atomic absorption cross section.[10] The resultant $\chi(k)$ versus k is shown in Fig. 2. $\chi(k)$ is Fourier transformed with the magnitude of the transform depicted in Fig. 3 along with the filter function which is used to isolate a particular coordination shell. A complex back-Fourier transform of the filtered signal is then taken with the amplitude and phase obtained as previously described[9] and shown in Fig. 4(a) and 4(b).

The phase and amplitudes obtained as described above were then used for a variety of comparisons. The phases were used to check phase transferability by using the total phase $2k\bar{r}_{AB} + \phi_{AB} + \sum_{AB}(k, \bar{r}_{AB}, T)$ and known $\bar{r}_{AB}$ from one system to determine $\bar{r}'_{AB}$ in another system which has the same absorbing atom A and scattering atom B. This also included comparisons between the same material at room temperature and 77 K, as shown in Fig. 5. The fitting procedure to obtain the best $\bar{r}_{AB}$ has been described elsewhere.[1,9] Here we only note that the use of a variable k scale

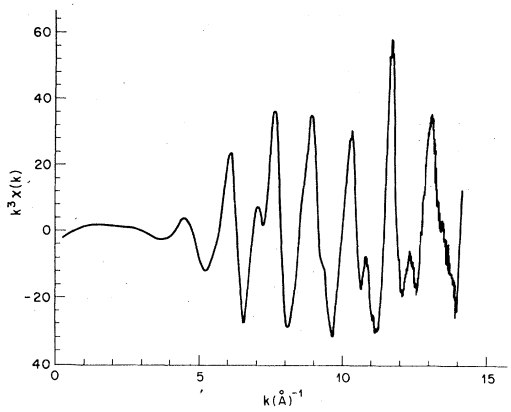

FIG. 2. $k^3\chi(k)$ for copper metal at 77 K.

(i.e., variable threshold energy) provides a certain degree of compensation for chemical-bonding variations. Such compensation is not available for chemically induced variation in the amplitude. We also note that $\phi_{AB} + \sum_{AB}(k, \bar{r}_{AB}, T)$ is only approximately 10% of the total phase and thus a 10% error in their determination will only cause a 1% error in $\bar{r}_{AB}$. However, 10% changes in $f(k, \pi)$, S_{AB}, and A_{AB} will directly cause a 10% change in the coordination number N_B.

In analyzing the amplitudes to test for transferability, one must make certain simplifying assumptions in order to hope to have a generally applicable approach. The procedure adopted for evaluating amplitude transferability in the well-characterized systems studied here is the one originally suggested by Stern *et al.*[2] If one incorrectly assumes that $f_B(k, \pi)$, $E_A^M(k)$, $L_{AB}^M(k, \bar{r}_{AB})$ are transferable for systems having the same absorbing atom A and scattering atom B in the same coordination shell, and that $S_{AB}(k, \bar{r}_{AB}, T)$

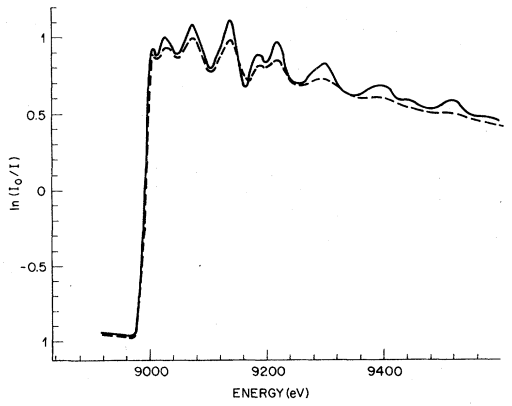

FIG. 1. Transmission spectrum of copper metal at 77 K (-) and RT (---).

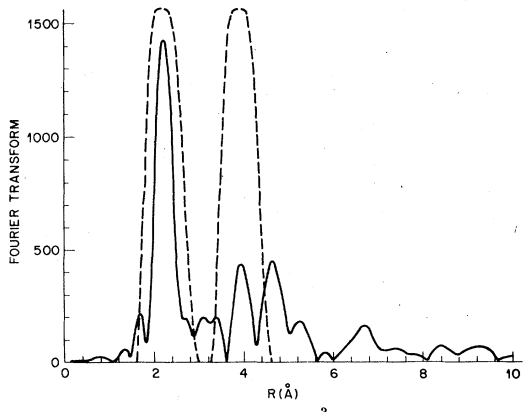

FIG. 3. Fourier transform of $k^3\chi(k)$ for copper metal at 77 K. The filters shown separate out the first and third shells, respectively.

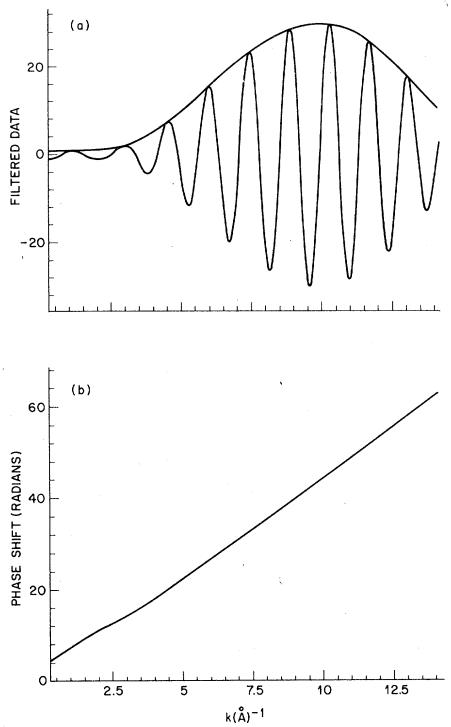

FIG. 4. (a) Filter $k^3\chi(k)$ of the first shell of copper metal at 77 K. Envelope is the amplitude of $k^3\chi(k)$. (b) Total phase of $k^3\chi(k)$ of the first shell of copper metal at 77 K.

$= e^{-2k^2\sigma^2} AB^{(T)}$ and $A_{AB}(k, \bar{r}_{AB}, T) = 0$, then

$$\ln\frac{|\chi_1(k)|}{|\chi_2(k)|} = \ln\frac{N_{1B}r_{2AB}^2}{N_{2B}r_{1AB}^2} + 2k^2(\sigma_{2AB}^2 - \sigma_{1AB}^2). \quad (5)$$

Therefore, if one plots the ln of the ratio of the amplitudes versus k^2, then the intercept at $k = 0$, I_{k_0} can be used to determine the coordination number in system one N_{1B}, if the coordination

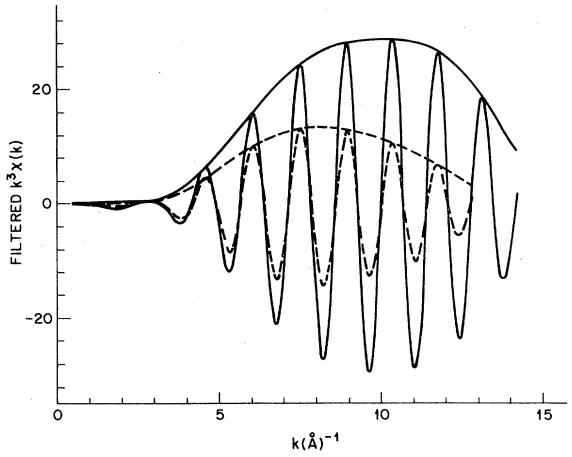

FIG. 5. Filtered $k^3\chi(k)$ and amplitude of $k^3\chi(k)$ for copper metal at 77 K (–) and RT (---).

number of system two N_{2B} is known, and if $\bar{r}_{1AB}$ and $\bar{r}_{2AB}$ are known. The experimentally determined value N_{1B} is given by

$$N_{1B}^E = (\ln^{-1} I_{k_0})\frac{N_{2AB}\bar{r}_{1AB}^2}{\bar{r}_{2AB}^2}. \quad (6)$$

The error in coordination-number determination is then given by

$$\Delta N = N_{1B}^E - N_{1B}. \quad (7)$$

While the percentage error is given by

$$\Delta N\% = \left(\frac{N_{1B}^E - N_{1B}}{N_{1B}}\right) 100. \quad (8)$$

The intercept I_{k_0} is obtained by making a best linear fit to the plot of $\ln|\chi_1(k)/\chi_2(k)|$ versus k^2. Due to the expected breakdown of the EXAFS formalism at low k and signal-to-noise and filter effects at high k, the linear fit was made over a limited region of the data. The region typically spanned from $k = 4$ Å to 11 Å^{-1}.

The accuracy of that determination is obtained by determining linear fits which have roughly twice the deviation of the best fit and using the I_{k_0} from those fits to find new ΔN and new $\Delta N\%$. Examples of such fits are shown in Fig. 6(a). The accuracy of the determination of $\Delta N\%$ will be denoted by $\pm\Delta E\%$ where

$$\Delta E\% = (\Delta N\%)_{\mathrm{BF}} - (\Delta N\%)_2, \quad (9)$$

where BF stands for best fit and subscript 2 for the fit with about twice the deviation. The same Cu sample was measured twice with each run independently analyzed. The two amplitude functions were indistinguishable. Thus we conclude that the data analysis does not significantly contribute to $\Delta E\%$.

Of course, in principle, Eq. (4) would yield

$$\ln\left|\frac{\chi_1(k)}{\chi_2(k)}\right| = \ln\frac{N_{1B}\bar{r}_{2AB}^2}{N_{2B}\bar{r}_{1AB}^2} + \ln\frac{f_{1B}(k,\pi)}{f_{2B}(k,\pi)} + \ln\frac{E_{1A}^M T L_{1AB}^M(k,\bar{r}_{1AB})}{E_{2A}^M T L_{2AB}^M(k,\bar{r}_{2AB})} + \ln\frac{(S_{1AB}^2 + A_{1AB}^2)^{1/2}}{(S_{2AB}^2 + A_{2AB}^2)^{1/2}}, \quad (10)$$

which obviously has many possible sources for producing ΔN and $\Delta N\%$. The systems chosen for this study are intended to separate out the relative contributions of the various factors.

For the experimental results which follow, we have tried to minimize various systematic efforts which would bias the data. In the area of data analysis, we have been completely successful. We have attempted to minimize and keep constant the finite energy-resolution corrections.[10] Sample integrity was verified by the matching of the ob-

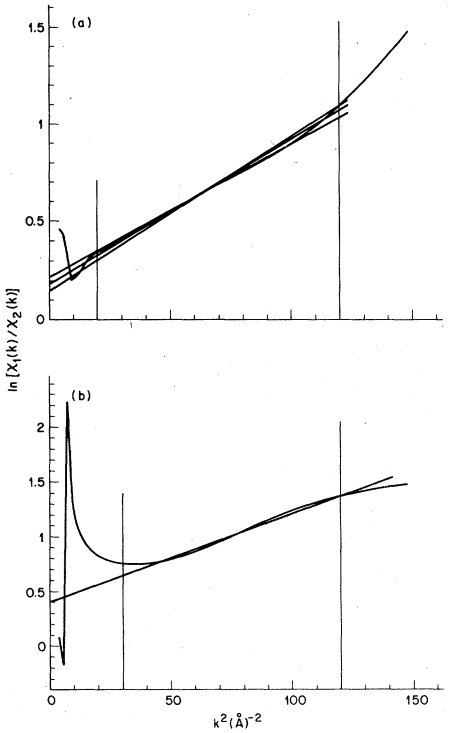

FIG. 6. (a) $\ln\chi_1(k)/\chi_2(k)$ as a function of k^2 with (1) being first shell of copper at 77 K and (2) being first shell of copper at RT. The middle straight lines represent the best fit and is used to determine I_{k_0} with the other two on either side being used to determine ΔN. The vertical lines represent the region over which the fit is made. (b) $\ln\chi_1(k)/\chi_2$ as a function of k^2 with (1) being third shell of copper at 77 K and (2) being third shell of copper at RT.

served shells in the EXAFS Fourier transform with the known distances. However, the possibility does exist in a study of this size that isolated errors may have been made and therefore we encourage anyone interested in a particular system to repeat the measurement for his own use.

III. EXPERIMENTAL RESULTS

There are four general types of comparisons that have been made using the data from the over twenty simple compounds measured in this study. They are the following: (1) Distance determinations using the experimentally determined phase systems with the same absorbing atom A and scattering atom B. (2) Nearest-neighbor and next-nearest-neighbor coordination-number determinations using the room-temperature amplitude as the model $|\chi_2(k)|$ and the 77 K amplitude in the same sample as the unknown $|\chi_1(k)|$. (3) Nearest-neighbor and more distant coordination-number determinations among pairs of substances which have the same absorbing atom A and same chemical type of atom B in the same coordination shell. All these comparisons are made using the low-temperature data. (4) Nearest-neighbor coordination-number determinations among pairs of systems which have the same scattering atoms B but different absorbing atoms A and the same crystal structure. Again, all comparisons are made using 77 K data.

Before describing the results of the four studies, it would be helpful to present the goals of each study. Study (1) has as its main purpose the verification that the family of systems chosen for this study do possess sufficient phase transferability to allow distance determinations to be made accurately. This means that both the pair-distribution function $g_{AB}(r)$ and the chemical environment are sufficiently regular that correct distances can be determined.[6] It also serves as an independent check for the presence of any systematic errors in the data. Study (2) is intended to evaluate the impact in these well-characterized systems of non-Gaussian and/or nonsymmetric disorder in coordination-number determinations. Study (3) is made at low temperature to remove the problems encountered in study (2) (i.e., a Gaussian should be a good approximation at 77 K) and has as its goal the evaluation of the impact of $f(k,\pi)$ and $TL^M(k,\bar{r}_{AB})$ on coordination-number determinations. Finally, study (4) is intended to evaluate the sensitivity of $E_A(k)$ and $L_A(k)$ to the atomic number of atom A and therefore indirectly the chemical sensitivity of those factors.

Study (1) involved the use of the empirically determined phases to determine interatomic distances. Over a hundred such determinations were made. The results of the testing of phase transferability and the resultant distance determinations in all the systems studied here are in complete accord with all previous studies. Namely, the distances determined using one AB system as a model for the whole family of AB systems resulted in distance determinations to accuracy of better than 0.02 Å for all low-temperature measurements, except for $KMnO_4$ where the distance disagreed by +0.08 Å from the x-ray determined value.[11] This included the case of insulators as well as metals and of comparing the same system at 77 K and room temperature. These results clearly show that, except possibly for the previously discussed case, none of the systems studied have large enough non-Gaussian or nonsymmetric disorders to require a corrective procedure to obtain the correct distances to 0.02-Å accuracy. Secondly, it demonstrates, of course, that chemical transferability is a valid concept to about 1% accuracy for distance deter-

minations. This in turn means that on the order of 10%, ϕ_{AB} itself is chemically transferable.

The results of the temperature study, study (2), are broken up into two parts, nearest neighbors and more distant coordination shells. The values obtained for ΔN, $\Delta N\%$, and $\%E$ for a representative group of systems are shown for the two cases in Tables I and II. A representative example of the data obtained for these two cases is shown in Figs. 5, 6(a), and 6(b). The trend is immediately obvious. If there is a significant error in coordination-number determination, it is that the room-temperature amplitude is too small or, of course, that the low-temperature result is too large. On the basis of Eq. (2), the first interpretation appears more likely for reasons we will now discuss. First, we assume that at 77 K, $e^{-2k^2\sigma_{77}^2}$ is a good representation (certainly relative to room temperature) of the Fourier transform of the pair correlation function. At room temperature, however, one has some small but finite non-Gaussian nonsymmetric disorder caused by the small-r hardness of the potential and the larger-r softness of the potential.[6] Thus at room temperature (RT) one might expect that

$$[S^2(k)+A^2(k)]^{1/2} \cong e^{-2k^2\sigma^2}\left(\alpha+\sum_n B_n k^{2n+1}\right). \quad (11)$$

Here $\alpha<1$ due to the loss of the high-disorder large-r part of the distribution which has decayed already by $k=4$ Å^{-1}. $\sum_n B_n k^{2n+1}$ represents the increasingly significant contribution (relative to the Gaussian part) of the sharp part of the pair distribution to the amplitude at high k. The ln of ratio of the 77 K to the RT data, then, has the following characteristics assuming for the moment that $\bar{r}_{77}=\bar{r}_{RT}$

$$\ln\left|\frac{\chi_1(k)}{\chi_2(k)}\right| = +2k^2(\sigma_{RT}^2-\sigma_{77\,K}^2) - \ln\alpha + \sum_n B_n k^{2N+1}.$$

Thus two effects cause N_{77}^E to be too large. At $k=0$, instead of giving zero, the result is $-\ln\alpha$ which, since $\alpha<1$, means that the $\ln^{-1}(I_{k_0})$ is greater than 1. Second, the slope at high k becomes less steep than expected on the basis of a simple Gaussian. This also increases the empirical value determined for I_{k_0} by the fitting procedure used in this study. Thus both effects cause N_{77}^E to be greater than the true coordination number. Their absolute contributions are hard to evaluate. A clue, however, to their relative contribution is provided by the larger errors observed for the distant-neighbor shells. This would suggest that it is the loss of contribution of the broad non-Gaussian part of the distribution, $\alpha<1$, which is dominant. For that shell correlations are reduced and $g(r)$ would be expected to have long tails and no significant sharp component. This latter interpretation is also consistent with the accurate distance determinations. Since the broad part does not contribute in the region in which the phases are used for distance determinations (i.e., $k<4$ Å^{-1}), they would not affect those determinations. One further point deserves mentioning. As seen experimentally and predicted by Eq. (5), there is in many cases a significant region of intermediate k where a good straight line exists and the change in the Gaussian part of the pair correlation function can be evaluated. The model developed here to rationalize our observations further suggests that two systems which have the same σ_{AB} for their Gaussian components might have other components whose character and size might be significantly different. Such a situation

TABLE I. Nearest-neighbor amplitude-temperature transferability results. ΔN, $\Delta N\%$, and $\Delta E\%$ are defined by Eqs. (7), (8), and (9), respectively.

	ΔN	$\Delta N\%$	$\Delta E\%$
$K_3Fe(CN)_6$	−0.18	−3	±3
$K_4Fe(CN)_6$	−0.18	−3	±3
Ferrocene	+0.9	+9	±2
MnO	0	0	±10
MnO_2	+0.4	+6	±4
NiO	0	0	±3
Cu_2O	+0.04	+2	±3
CoS	+0.4	+6	±5
CoS_2	+0.2	+3	±5
NiS_2	+0.12	+2	±3
CuCl	+0.8	+20	±5
Cu	+2	+14	±3
Ni	+1	+9	±3

TABLE II. Amplitude-temperature transferability results for more distant shells. ΔN, $\Delta N\%$, and $\Delta E\%$ are defined by Eqs. (7), (8), and (9), respectively.

	Shell	ΔN	$\Delta N\%$	$\Delta E\%$
MnO	2	0	0	±3
CoO	2	+0.6	+10	±2
NiO	2	0	0	±3
ZnO	2	+1	+8	±3
NiF_2	3	+1	+12	±3
$NiSi_2$	2	+2.4	+20	±5
CoS_2	2	+0.4	+3	±3
NiS_2	2	+1.8	+15	±5
Ni	3	+0.9	+15	±5
Cu	3	+2.4	+40	±5
Cu_2O	2	+5	+35	±5

would adversely affect empirical coordination-number determinations.

The lesson learned from this study is that for amplitude determinations one should make measurements at low temperature. Otherwise errors as large as 10% can be made in coordination-number determinations for nearest neighbor or 20% for more distant neighbors.

The comparison of low-temperature amplitudes between different systems with the same absorbing atom A and same atom B in either the nearest-neighbor or more distant coordination shells, study (3), is of course the most direct test of chemical transferability. The results of those comparisons are shown for the nearest-neighbor case in Table III and for the distant-neighbor case in Table IV.

There are two trends in the data in Table III. The first trend is that when atom B is a first-row element, amplitude transferability is poorer. The second trend is that the presence of other chemically dissimilar atoms in systems with the same nearest neighbor AB pair also adversely affects amplitude transferability. An example of the combined effect of both factors is shown in Fig. 7. Note for this figure and succeeding ones that to facilitate direct comparisons of amplitudes, the $\chi(k)$ data have been renormalized by multiplying by $\bar{r}_{AB}^2$ and dividing by N_B. Thus the normalized amplitudes are per scattering atom at a unit distance. For Fig. 7 one can see the similarity of the shapes for $K_4Fe(CN)_6$ and $K_3Fe(CN)_6$ but the differences with ferrocene. The effect of the different shapes on coordination-number determinations is illustrated in Fig. 8. A similar effect holds for the series MnO, MnO_2, and $KMnO_4$, with $KMnO_4$ again being very different in shape. An example of the opposite case, same chemical constituents, and a second-row element is shown in Figs. 9 and 10. The regularity of the normalized amplitude shapes in Fig. 9 is obvious and the accuracy of the resulting amplitude transferability is shown in Fig. 10. It can also be observed from Figs. 8 and 10 that the amplitudes have a significant variation with chemical changes in the low-k region. What is slightly surprising is that these effects seem to extend out to $k = 5 - 6$ Å^{-1} in many cases. Inclusion of lower-k data for coordination-number determinations could result in serious errors. This of course is also a contributing factor to the amplitude difficulties with low-atomic-number scatterers where the $f(k, \pi)$ drops off so quickly that one usually has information that extends only out to 10 Å^{-1}. At first glance the sensitivity of the first-row element would also appear to be a reasonable trend since they have the highest percentage of chemically sensitive elec-

TABLE III. Amplitude-transferability results for nearest neighbors in systems with the same type absorbing atom A and scattering atom B. ΔR is the difference in interatomic distance between the model and the "unknown". ΔN, $\Delta N\%$, and $\Delta E\%$ are defined by Eqs. (7), (8), and (9), respectively.

Model	Unknown	ΔR	ΔN	$\Delta N\%$	$\Delta E\%$
$K_3Fe(CN)_6$	$K_4Fe(CN)_6$	0	−0.48	−8	±2
Ferrocene	$K_4Fe(CN)_6$	+0.14	+0.6	+10	±4
$K_3Fe(CN)_6$	Ferrocene	−0.14	1.6	−16	±4
MnO	MnO_2	+0.34	+0.06	1	±5
$KMnO_4$*	MnO_2	−0.34	+2.7	+45	±10
MnO	$KMnO_4$*	0.68	−1.2	−30	±10
Cu_2O	CuO	0.03	0.4	10	±5
CoS	CoS_2	−0.01	0.2	3	±3
CuCl	$CuCl_2$	−0.01	−0.12	−3	±2
Ni_5Y	Ni	−0.06	0.12	1	±3
Ni_5Pr	Ni	−0.06	1.7	14	±10
Ni_5Y	Ni_5Pr	0	+0.69	16	±10

TABLE IV. Amplitude-transferability results for more distant shells in systems with the same absorbing atom A and scattering atom B in the shell being studied. ΔR is the difference in interatomic distance between the model and the "unknown". ΔN, $\Delta N\%$, and $\Delta E\%$ are defined by Eqs. (7), (8), and (9), respectively.

Model	Shell	Unknown	Shell	ΔR	ΔN	$\Delta N\%$	$\Delta E\%$
$NiSi_2$	2	NiS_2	2	−0.19	−5.40	−55	20
NiS_2	2	Ni	3	−0.40	96	+400	100
$NiSi_2$	2	NiF_2	2	+0.19	+1.28	+16	15
NiF_2	3	NiO	2	+0.13	2	+16	10
MnF_2	2	MnO_2	2	+0.40	−2.40	−30	5
MnF_2	2	MnO	2	+0.68	0	0	7
MnO	2	MnO_2	2	−0.28	−2.6	−33	5
CoO	2	CoF_2	2	−0.66	−1	−12	5
CoS_2	2	CoF_2	2	+0.23	+10	+123	20
CoS_2	2	CoO	2	+0.89	+17	+150	10

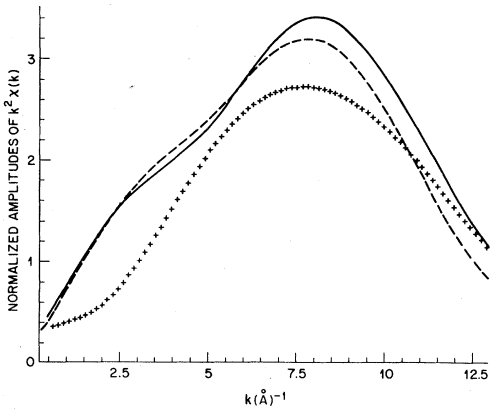

FIG. 7. The first shell of $K_4Fe(CN)_6$ (-), $K_3Fe(CN)_6$ (---), and ferrocene (+++) all at 77 K. Normalization achieved by multiplying $k^2\chi(k)$ by $\bar{r}_{AB}^2$ and dividing by N_B.

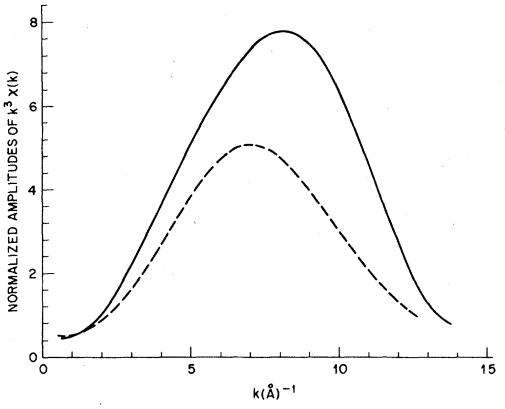

FIG. 9. Normalized amplitude $k^3\chi(k)$ for CoS_2 (-) and CoS (---), respectively. Normalization achieved by multiplying $k^3\chi(k)$ by $\bar{r}_{AB}^2$ and dividing by N_B.

trons. Only the two 1s electrons can be considered to be chemically insensitive, though even they are more deeply bound in atoms with higher atomic numbers. This line of reasoning would suggest that $f(k,\pi)$ itself is not transferable, a point somewhat refuted by the transferability of ϕ_{AB}. It was previously mentioned, however, that ϕ_{AB} would be considerably less transferable if the threshold energy were not allowed to vary. This variation of the choice of threshold has a much more significant effect on distance determination when B is a first-row element because then the EXAFS intensity does not go out to high k because of the just discussed relatively rapid falloff of $f(k,\pi)$ for the low-Z elements. Also, one should remember that the high-k data play the dominant role in distance determination while the low-k data are more important for the coordination-number determination. This is because the distance is found by the determination of a slope while the coordination number is determined by the value of the intercept at $k=0$. The value of a slope for a line passing through the origin is most influenced by the high-k part of the line while the value of an intercept is more sensitive to the low-k part of a line. Of course the low-k data are more affected by the weakly bound chemically sensitive electrons than the high-k data where one is essentially getting only contributions from the tightly bound core electrons. This discussion should not be confused to mean that the whole effect is due to $f(k,\pi)$, but rather that it may cause the distinction observed in this limited study for the first low elements. The sensitivity to the presence of other chemically dissimilar atoms clearly implicates $L^M(k,\bar{r}_{AB})$ as contributing to the lack of transferability.

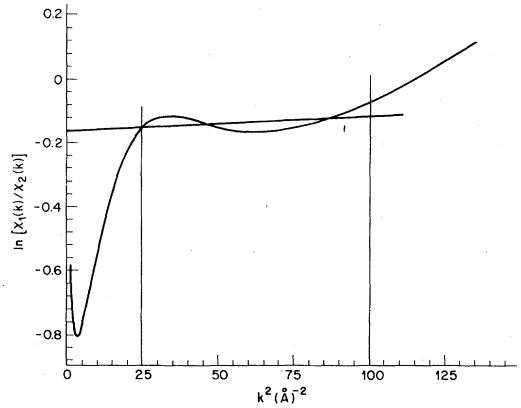

FIG. 8. $\ln\chi_1(k)/\chi_2(k)$ as a function of k^2 with (1) being the normalized first shell of ferrocene at 77 K and (2) being the normalized first shell of $K_3Fe(CN)_6$ at 77 K.

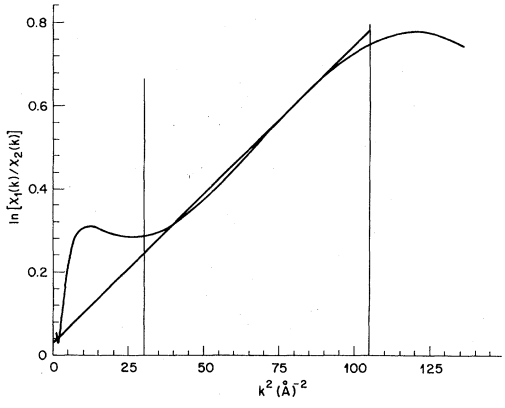

FIG. 10. $\ln\chi_1(k)/\chi_2(k)$ as a function k^2 with (1) being the normalized first shell of CoS_2 at 77 K and (2) being the normalized first shell of CoS at 77 K.

The fact that $TL^M(k,\bar{r}_{AB})$, itself, is also not transferable is more clearly shown in Table IV where the results of chemical transferability for the more distant-neighbor coordination shells are shown. Clearly very large deviations are observed for the cases studied, all of which are for when both A and B are transition metals. $f(k,\pi)$ should be transferable for these systems and since they were measured at 77 K the distribution function should be Gaussian. There is also a notable absence of a trend with the atomic number of the nearest-neighbor coordination shell suggesting as expected that it is the loosely bound electrons which affect the losses. All this suggests $TL^M(k,\bar{r}_{AB})$ as the cause of the lack of transferability.

The effect of $TL^M(k,\bar{r}_{AB})$ on the amplitude shapes is illustrated in Fig. 11 and on coordination-number determinations in Fig. 12. The absence of a systematic trend between the sign of ΔN and ΔR in Table IV for any series of results involving the same atoms (i.e., Ni–Ni, etc.) clearly demonstrates that $TL^M(k,\bar{r}_{AB})$ cannot be represented by the simple form $e^{-2\bar{r}_{AB}/\lambda(k)}$. One cannot rule out the functional form $e^{-2\bar{r}_{AB}/\lambda^M(k)}$ where both $\bar{r}_{AB}$ and $\lambda^M(k)$ can vary from one system to another. However, as discussed previously there is no reason to believe that $TL^M(k,\bar{r}_{AB})$ is better described by such a functional form than others with the same number of independent parameters. The results in Tables III and IV taken together also suggest that it is $L^M(k,\bar{r}_{AB})$ and not $L_A^M(k)$ and $L_B^M(k)$ which is causing the dominant variation. The major trend supporting this conclusion is the significantly worse results obtained for the distant shells relative to the nearest-neighbor case. However, the contributions cannot and need not be quantitatively separated for this study.

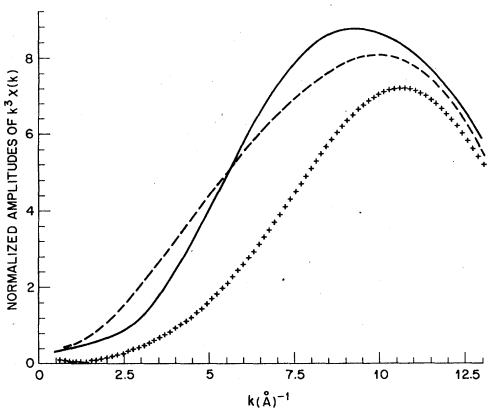

FIG. 11. Normalized amplitudes of $k^3\chi(k)$ for the second shell of CoO (–), CoF_2 (---), and CoS_2 (+++) all at 77 K. Normalization achieved by multiplying $k^3\chi(k)$ by $\bar{r}_{AB}^2$ and dividing by N_B.

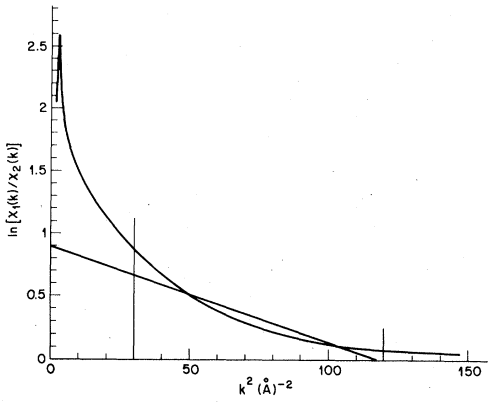

FIG. 12. $\ln\chi_1(k)/\chi_2(k)$ as a function of k^2 with (1) being the normalized second shell of CoF_2 at 77 K and (2) being the normalized second shell of CoS_2 at 77 K.

The conclusions we derive from study (3) are that chemical-amplitude transferability is most reliable for the case of high-Z nearest neighbors in compounds with identical chemical constituents. For those cases it is better than 10%. We also observed that it can be appreciably worse, 30% for first-row nearest neighbors in chemically dissimilar substances, and as large as factors of 2 for more distant neighbors, even after some first-order correction for the distance difference. One has also observed that $f(k,\pi)$ and $TL_{AB}^M(k,\bar{r}_{AB})$ vary with chemical environment.

The results of study (4) involving materials with the same crystal structure and number and chemical type of scattering atoms but a different transition-metal-absorbing central atom is shown in Table V. The effect of the different central atoms and consequently different valence-charge distributions on the amplitudes is shown in Fig. 13. The lack of any systematic trend with the atomic num-

TABLE V. Amplitude-transferability results for nearest neighbors in systems with the same crystal structure and same scattering atom B but different absorbing atoms A. ΔR is the difference in distance between the model and the "unknown". ΔN, $\Delta N\%$, and $\Delta E\%$ are defined by Eqs. (7), (8), and (9), respectively.

Models	Unknown	ΔR	ΔN	$\Delta N\%$	$\Delta E\%$
CoO	NiO	0.05	3.9	65	±10
MnO	NiO	0.14	0.3	5	±5
MnO	CoO	0.09	−2.71	−45	±10
CoF_2	NiF_2	0.04	+1.5	25	±5
MnF_2	NiF_2	0.11	+1.0	17	±5
MnF_2	CoF_2	0.07	−3.0	−5	±5
CoS_2	NiS_2	−0.08	−1.0	−17	±5

ber of atom A in various structural series studied suggests that it is the differences in bonding which are causing the dominant variation. The variation of $E_A^M(k)$ and $L_A(k)$ indicated in this study seems to be at least as great as that found in the previous study. Again it is impossible on the basis of this study to separate out the effects of $E^A(k)$ and $L^A(k)$.

Even prior to this study one would probably not have believed that EXAFS amplitudes could be used for chemical identification among neighboring elements, but one might have been tempted to say they could be used to distinguish between neighboring rows. The first belief is strongly supported by Fig. 14 in which the normalized first-shell amplitudes for NiF_2 and NiO are shown to be as similar as for those materials with the same AB pair which are depicted in Fig. 7. The second belief was based primarily on the distinctly different range and shape of $f(k, \pi)$ for atoms with significantly different atomic numbers. This belief is supported by this study for nearest neighbors as shown by Fig. 15 in which the nearest-neighbor amplitudes for NiS_2 and Ni metal are shown. The only exception to this could arise if $g(r)$ for the case of a high-atomic-number atom B was very broad, then it might look within the variations that exist in the shapes of the first-row atoms like a first-row atom. Also the results shown in Figs. 11 and 16 when compared with those of Fig. 15 indicate that even in highly ordered systems a similar effect can occur for the more distant shells due to distortions in shape caused by $TL^M(k, \bar{r}_{AB})$.

IV. DISCUSSION

The presence of many factors in the amplitude expression for the EXAFS amplitude, each of which has the potential of chemical sensitivity, should in itself be regarded as a warning signal in the use of EXAFS for coordination-number determinations. The studies reported here show that most of the factors do, in fact, vary in going from one chemical system to another. This has explicitly been shown to be the case for $S_{AB}(k, \bar{r}_{AB}, T)$, $A_{AB}(k, \bar{r}_{AB}, T)$, $f_B(k, \pi)$, $E_A^M(k)$, and $TL_{AB}^M(k, \bar{r}_{AB})$. Since these factors depend upon the chemical environment, it is certainly impossible to calculate them for an unknown system, and even extremely difficult to calculate them for a known chemical system. A notable exception to this might be simple molecules.[12] In the absence of explicit calculations, one might be tempted to derive a functional form for each factor and then fit the observed amplitude to determine both the coefficients of those functional forms and the co-

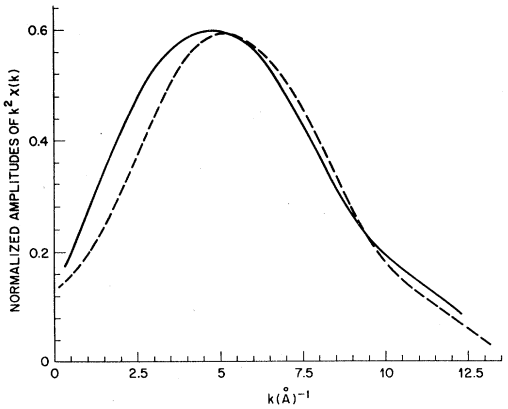

FIG. 14. Normalized amplitudes of $k^2\chi(k)$ for the first shell at 77 K of NiF_2 (-) and NiO (---).

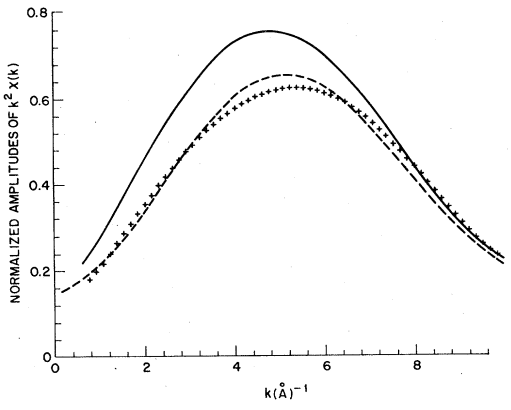

FIG. 13. Normalized amplitude of $k^2\chi(k)$ for the first shells at 77 K of NiF_2 (-), MnF_2(---), and CoF_2 (+++).

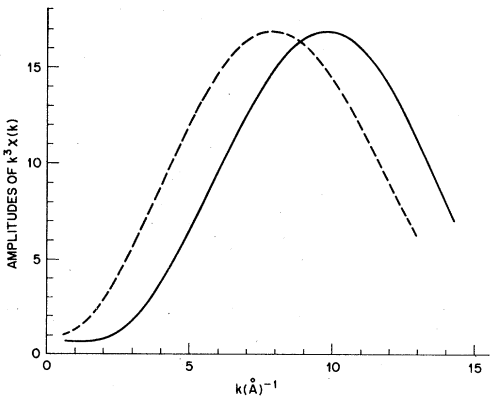

FIG. 15. Amplitude of $k^3\chi(k)$ for first shell at 77 K of Ni metal (-) and NiS_2 (---). The NiS_2 normalized amplitude was multiplied by 3.4 to make it the same size as the normalized amplitude of Ni.

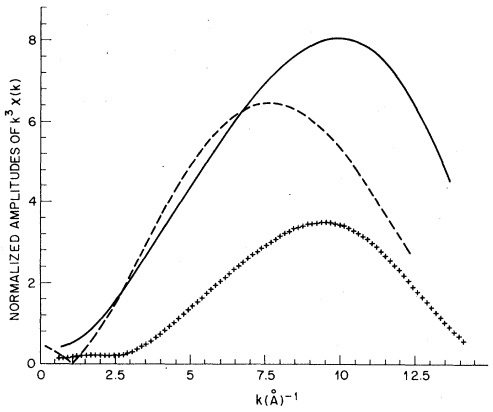

FIG. 16. Normalized amplitudes of $k^3\chi(k)$ for the second shells at 77 K of CoF_2 (–), MnF_2 (---), and NiF_2 (+++).

ordination number. There are several problems with the above approach. The first is that, for $k > 5$ Å^{-1}, it is likely that $E_A(k)$ is a constant and thus at best one could determine the product $N_B E_A(k)$. Secondly, one would expect significant correlations to exist between $N_B E_A(k)$ and variations allowed within the functional form for the product

$$f(k,\pi) T L^M_{AB}(k,\bar{r}_{AB})[S^2_{AB}(k,\bar{r}_{AB},T)+A^2_{AB}(k,\bar{r}_{AB},T)]^{1/2}.$$

Finally, there is the difficulty that with finite k range, resolution, and signal-to-noise, the number of independent parameters that the EXAFS amplitude can uniquely determine is severely limited.[13] The functional description of the various factors would more than likely require more parameters than can be determined uniquely from the data.

This leaves models as the most likely approach. Our work suggests that, even if one measures EXAFS at low temperatures, the requirements on the chemical similarity of the model become increasingly more stringent as one considers the cases of heavy-atom nearest-neighbor, first-row nearest-neighbor, and next-nearest-neighbor coordinations. With care, nearest-neighbor coordinations can be determined to better than 10% and next-nearest neighbors to 40%. The above does not mean that the determination cannot be more accurate, but it does mean that because of the complexity of the phenomena which contribute to the amplitude, the possibility exists that there is a significant systematic error. This danger obviously becomes greater the less one knows about the chemical state of the system being studied. An example of such a case is the use of bulk samples as models for surface EXAFS. This already has been recognized to have given problems with nearest-neighbor coordination-number determinations. The cause of the problem was attributed to the variation in $TL^M_{AB}(k,\bar{r}_{AB})$.[14] The solution to that problem decided on by workers in the field is to use the polarization dependence together with a limited number of geometrical alternatives to determine the site and, therefore, the coordination number. Using the system itself as the model obviously will minimize all the difficulties discussed in this work. Others[7] have used similar approaches to study the changing properties of a system. Such studies are likely to be the most reliable for coordination-number determinations. As examples they indicate that the conclusions of this work must be tempered by the realization that many studies will be able to successfully determine the desired structural features without direct utilization of amplitude transferability.

ACKNOWLEDGMENTS

We would like to thank the always helpful operations staff of the Stanford Synchrotron Radiation Laboratory. One of us (P. E.) would like to acknowledge many stimulating discussions with P. A. Lee and B. M. Kincaid.

[1] P. H. Citrin, P. Eisenberger, and B. M. Kincaid, Phys. Rev. Lett. 36, (22) 1346 (1976).
[2] E. A. Stern, D. E. Sayers, and F. W. Lytle, Phys. Rev. B 11, 4836 (1975).
[3] S. P. Cramer, K. O. Hodgson, W. O. Gillum, and L. E. Mortenson, J. Am. Chem. Soc. 100, 2298 (1978).
[4] G. S. Brown, P. Eisenberger, and P. Schmidt, Solid State Commun. 24, 201 (1977).
[5] P. A. Lee and G. Beni, Phys. Rev. B 15, 2862 (1972).
[6] P. Eisenberger and G. S. Brown, Solid State Commun. 29, 481 (1979).
[7] J. B. Boyce, T. M. Hayes, W. Stutius, and J. C. Mikkelsen, Jr., Phys. Rev. Lett. 38, 1362 (1977).
[8] J. J. Rehr, E. A. Stern, R. L. Martin, and E. R. Davidson, Phys. Rev. B 17, 560 (1978).
[9] P. Eisenberger and B. M. Kincaid, Science 200, 1441 (1978).
[10] B. Lengeler and P. Eisenberger, Phys. Rev. B 21, 4507 (1980).
[11] S. Ramaseshan, K. Venkatesan, and N. V. Mani, Proc.

Indian Acad. Sci. 46A, 95 (1957).
[12]E. A. Stern, S. M. Heald, and B. Bunker, Phys. Rev. Lett. 42, (20) 1372 (1978).
[13]P. A. Lee, P. Citrin, P. Eisenberger, and B. M. Kincaid, Rev. Mod. Phys. (1980) (in press).
[14]P. Citrin, P. Eisenberger, and R. C. Hewitt, in Proc. of European Conference on Surface Science II [Surf. Sci. 89, 28 (1979)].